



INSTITUT DE FRANCE
Académie des sciences

Comptes Rendus

Chimie

Gérard R. Colmont, Dominique Bazin and Michel Daudon

SEM-EDX micro-analysis and FTIR infrared microscopy by ATR of a bladder stone from the IIIth millennium BC from the B1S passage-grave of the necropolis in Chenon (Charente, France)


Volume 25, Special Issue S1 (2022), p. 431-444

Published online: 14 January 2022

<https://doi.org/10.5802/crchim.143>

Part of Special Issue: Microcrystalline pathologies: Clinical issues and nanochemistry

Guest editors: Dominique Bazin (Université Paris-Saclay, CNRS, ICP, France), Michel Daudon, Vincent Frochot, Emmanuel Letavernier and Jean-Philippe Haymann (Sorbonne Université, INSERM, AP-HP, Hôpital Tenon, France)

 This article is licensed under the
CREATIVE COMMONS ATTRIBUTION 4.0 INTERNATIONAL LICENSE.
<http://creativecommons.org/licenses/by/4.0/>



Les Comptes Rendus. Chimie sont membres du
Centre Mersenne pour l'édition scientifique ouverte
www.centre-mersenne.org
e-ISSN : 1878-1543



Microcrystalline pathologies: Clinical issues and nanochemistry / *Pathologies microcristallines : questions cliniques et nanochimie*

SEM-EDX micro-analysis and FTIR infrared microscopy by ATR of a bladder stone from the IIIth millennium BC from the B1S passage-grave of the necropolis in Chenon (Charente, France)

G rard R. Colmont^{ *,a}, Dominique Bazin^{ b} and Michel Daudon^{ c}

^a Honorary Professor of Biology, PhD of Archaeology from EHESS, Paris, France

^b Universit  Paris-Saclay, CNRS, Institut de Chimie Physique, 91405, Orsay, France

^c Laboratory of Physiology and INSERM Unit UMRS 1155, Tenon Hospital, Paris, France

Current address: 66 bis Rue des Saules F-33500 Libourne, France (G. R. Colmont)

E-mails: colmont.gerard@wanadoo.fr (G. R. Colmont),

dominique.bazin@universite-paris-saclay.fr (D. Bazin), daudonmichel24@gmail.com (M. Daudon)

Abstract. Here is a case of bladder stone of average size dated to the Late Neolithic period, found in the multiple burial of the B1S passage-grave in Chenon (Charente, France). Chemical analysis showed a mixed composition. The core, intermediate and surface envelopes consist in calcium phosphate apatite associated with whitlockite and amorphous carbonated calcium phosphate, all clarified by Fourier Transform InfraRed spectroscopy. Calcium phosphatic stones are characteristic of communities, such as those of the Neolithic period, where the diet was rich in cereal carbohydrates and poor in animal proteins. The excavation of such extra-skeletal objects is an event that is particularly interesting as it provides documents on the history of diseases and diets in ancient populations. The complete set of data suggests that this bladder stone was formed during a urinary tract infection with a germ possessing a very active urease.

Keywords. Infectious stone, Carapatite, Whitlockite, Amorphous carbonated calcium phosphate, FTIR spectroscopy, Microchemical analysis, Urease.

Published online: 14 January 2022

1. Introduction

The graves do not only contain skeletal remains and offerings accompanying the deceased. Calcified

extra-skeletal objects can also be found there such as bladder stones or kidney stones, gallstones, prostatic and pancreatic stones, uterine and gastrointestinal leiomyomas, ovarian cysts, ovaries, fetus, lymph node, etc. [1–6].

* Corresponding author.

Urinary lithiasis (from the Greek *lithos*, stone) is one of the major pathologies in which environmental factors play a major role. It was widespread in ancient populations [7,8] and dates back at least to the Paleolithic Age, as evidenced by the discovery of a urinary stone dated to about 8500 years BC in a Mesolithic cave on the Sicilian coast [9,10]. As early as 1797, Wollaston described urinary stone components as magnesium and ammonium phosphate in his publication entitled “On gouty and urinary concretions” [11]. By the end of the 18th century, the chemical composition of urinary stones was identified by chemists and physicians of the time. In addition to ammonium and magnesium phosphate, calcium phosphate, calcium oxalate, uric acid, ammonium urate, cystine, xanthine and even silica were found in stones, with major epidemiological differences compared to what is now known. Uric acid was more frequent in adults from well-to-do backgrounds, whereas phosphates were more prevalent in poorer populations and in children who were more exposed to malnutrition and urinary tract infections. Nowadays, in almost all countries of the world, the most common composition of stones is calcium oxalate.

Archaeological evidence has revealed that humans knew about kidney stones and, more important, knew how to treat them [12]. In 1550 BC, during the reign of Amenhotep I of the XVIIIth Dynasty, the Ebers Papyrus, about twenty meters long, relates the various remedies used in Pharaonic Egypt in 877 prescriptions, in particular those concerning the bladder diseases. The calculi are named *Oourmyt* [13]: the prescription recommended for “hunting” them is based on cow-milk or beer [14] (Eb 20 (6, 10–16)). In ancient Greece, Hippocrates pointed out the dangers of bladder stones and advocated urinalysis. Indian Sanskrit documents mention the removal of stones via the supra-pubic route [15]. During the reigns of Augustus and Tiberius, the Roman encyclopedist and physicist Aulus Cornelius Celsus described in his book *De Medicina* the symptoms of “stone disease” as well as the surgery to be used to extract bladder stones [16].

Studies have shown that bladder stones were a disease of communities where the diet was high in cereal carbohydrates and low in animal protein [17]. And we know that Neolithic populations were agricultural, that they had domesticated wild cereals,

but also that they practiced animal husbandry. Conversely, obesity due to a diet rich in animal proteins, nucleoproteins (offal, game) and fats may be the cause of the formation of other stones, including uric acid and calcium oxalate, a superinfection of the urinary tract by urease microorganisms that can transform uric acid into ammonium urate. This may explain rare observations in the literature such as the one reported in 2011 by Giuffra *et al.* [18] regarding a left kidney stone found in the mummy of an Italian nobleman in 15th century our era composed of ammonium urate with 5% weddellite. Several months before his death, the subject had developed an infection, presumably with a urinary tract origin. It led to sepsis that was responsible for his death [18]. It has even been considered that the risk of stone development may be related to seasonal changes in climate, increased ambient temperature [19] and the number of hours of sunlight per month [20], and therefore changes in body hydration and vitamin D metabolism.

The discoveries of biological calcifications dated to Prehistoric and early historical times are rare, which makes their analysis interesting. This was the case for a calcified tuberculous lymph node found under a dolmen near Carcassonne (Aube) in an archaeological layer from the Chalcolithic period [1, 21]. Likewise, a urinary bladder calculus with a diameter of 42 mm, composed of calcium phosphate, was discovered among the human bones of the Bertrandoune dolmen in Prayssac (Lot) dated 2200 years BC [21,22]. The sense of observation allowed Dr. E. Gauron in 1971–1972 to collect in the B1S passage-grave at Chenon (in its corridor?) a calcification, already reported [23], which will be considered below.¹ As urolithiasis can be due either to dietary errors [24–27] or to urinary tract infections [24,25,28,29], its study could possibly provide information on the diet of the populations of that time and their diseases as well as its history and its causes.

¹Dr. E. Gauron (†) was the director of the excavation of this passage-grave and at the same time the only physician in the team. This bladder stone was collected by him alone without being recognised. Being for some time the custodian of the human bones of this excavation, the main author of this article (GRC) noticed this “stone”, reported it in an article of a paper [23] and he had it analysed in order to know about its nature.

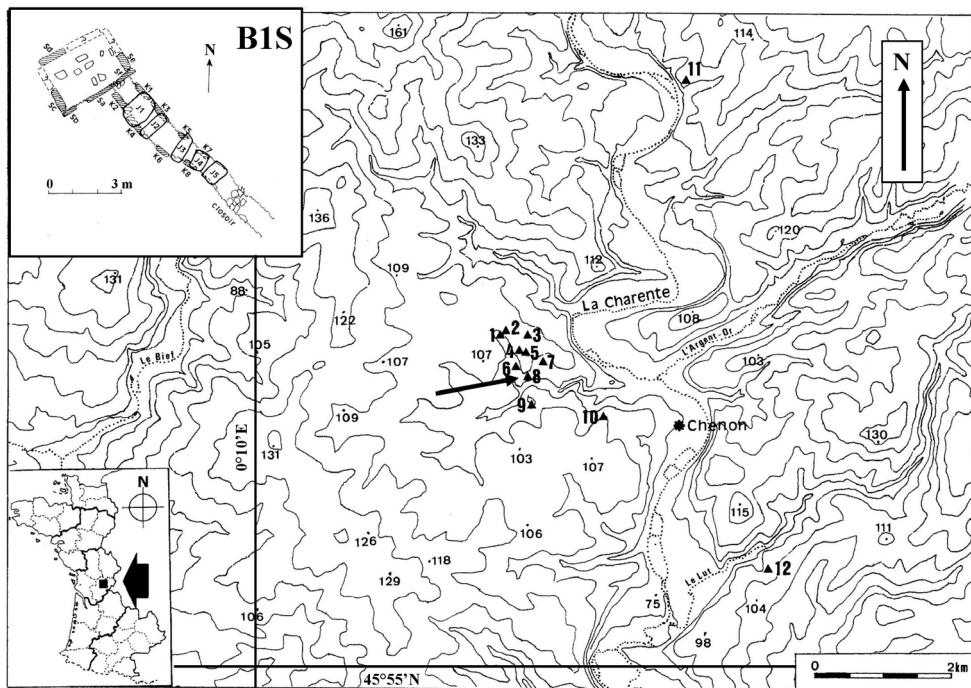


Figure 1. Monumental plan of the passage-grave B1S in Chenon (by Lotte [30]) with the topographic situation of the necropolis in Chenon (Charente, France) in its archaeological environment (on the IGN map of Ruffec in 1/50,000^e).

2. The study area. The archaeological context

At the time of its excavation, cairn B1 at Chenon (which contained the two passage-graves named B1S and B1T) had a sagging and oval appearance [30]. It was made up of more or less flat limestone and stones. S-chamber lacked the cover table. Its corridor was covered with five disjointed slabs (Figure 1). The dental MNI (Minimum Number of Individuals) made it possible to count twenty-nine adults and seventeen subadults in the S-chamber (eight young child, four older child, five adolescents), and fourteen subadults in the S-corridor (one infant, seven young child, four older child, two adolescents). It is the bone MNI (with the axis) that has been used to claim that twenty-four adult skulls have passed through the S-corridor [23].

Two absolute dates were obtained on human bone fragments collected respectively on the north side of the S-chamber and in half of the S-corridor near the chamber giving the 3rd millennium BC (Ly-17044: 3081 to 2896 cal BC at 2σ and Ly-17045: 3012 to 2888 cal BC at 2σ) as the period of deposit, i.e. the Early

Neolithic I period (according to Guilaine [31]) while bones of the deep layer of the T-chamber are related to an older period, the 5th millennium BC (Ly-1105: 4712 to 4040 BC at 2σ), i.e. the beginning of the Middle Neolithic (according to Guilaine, [31]) close to the period of construction of the monument.

The human skeleton has kept the marks of external aggressions, this during childhood and until adulthood. Thus, when the nutrient supply is not sufficient, it appears in the bones or teeth "biological stress" [32]. This stress can be seen by a more or less pronounced microporous aspect of the orbits [33] called *cribra orbitalia* (seen in the chamber of the B1T dolmen, [23]). In this specific case, some authors presently think about a vitamin B12 deficiency in the mother followed in childhood by a nutritional deficiency coupled with intestinal infections [34]. The other indicator of stress is dental enamel hypoplasia, which consists of a reduction in the thickness of the enamel appearing on the crown as parallel horizontal depressions but sometimes also as pits. There are a lot of causes of dental enamel hypoplasia:

genetic predisposition, nutritional deficiencies, infections, prematurity, high fever [35–38]. As with bladder or kidney stones, the study of linear enamel hypoplasia (LEH) is an essential tool for the reconstructing aspects of health in the past [39–42]. In these studies, the age at which this physiological stress occurred and its duration are still to be asserted [43], knowing that enamel grows non-linearly [44]. As the skeletal remains of children are generally under-represented in the archaeological record, the study of LEHs will be carried out in adults and will provide a historical account of childhood stress episodes for a particular region and time period [38]. Such hypoplasias were observed on permanent adult teeth in the corridor of the B1S passage grave (20 cases), mainly on upper lateral incisors and lower canines, and on permanent subadult teeth found in the chamber (one lower incisor) and in the corridor (one lower canine and one lower first premolar) of the B1S passage-grave [23].

All these studies and observations point to a better knowledge of the living conditions of populations in the past. We can already observe that a bad diet as well as diseases contracted sometimes in childhood leave traces in the skeleton.

3. Methods

At present, the diagnosis of calcified biological masses such as bladder stones remains a procedure widely used in medicine and paleopathology. First there are the conventional techniques which are morphological, radiographic and microscopic analyzes. Advanced techniques, for their part, consist of elementary microanalysis by energy dispersive X-ray analysis (SEM-EDX) and X-ray fluorescence (XRF) as well as chemical analysis through Powder X-ray diffraction (XRD) and Fourier Transform InfraRed spectroscopy (FTIR) to obtain information on the elementary and chemical composition of the different envelopes of the calculus and of its nucleus [45].

The different methods we have used in this investigation are obviously nondestructive one. First, imaging at the micrometer scale has been performed with a micro-scanner (GE V/tome/XS). The samples have been observed with two SEM in environmental mode to preserve it [46–48]. Observations have been performed by backscattered

electrons BSE (Zeiss EVO 50, SEM LaB6 at optimized variable pressure, 25 kV) and secondary electrons (field-emission “gun” Zeiss SUPRA 55-VP, at low voltage between 0.5 and 2 kV), on the surface, and in depth thanks to its section, with different magnifications (500× to 4500×), to detect crystals and identify them as well as to look for possible imprints of bacteria [28,29] that can be responsible for the formation of the calculus. X-ray microanalysis (EDX) done on the second electron microscope makes an elemental analysis by detecting the characteristic lines of the present chemical elements [29,46–48]. Finally, chemical analysis has been performed by attenuated total reflection ATR with the Spotlight 400 FTIR Imaging System from Perkin-Elmer. The spectral range adopted goes from 4000 to 520 cm^{-1} at a resolution of 16 cm^{-1} [49,50].

Such approach has been successfully applied to different kinds of concretions including kidney [51–53], prostatic [54,55] and pancreatic [56] stones and in the case of two giants bladder stones found in the pelvis of a sixteenth–seventeenth century adult as well [57].

Thus, these various observations and analyzes will make it possible to analyze and define, with the maximum of supporting evidence, the nature of this calculus and, if possible, its cause.

4. Analysis and results

The preliminary remarks of Gauron and Mas-saud [30] suggest the risks of pollution of the funeral deposit by the external environment with the consequence of a modification of its physicochemical characteristics of origin. Rather, if this bladder stone was collected in the archaeological layer of the S-corridor (and not outside) that is relatively thick of 54 cm, then these “pollutions” were very reduced, and that would be good news.

This calcification appears in a slightly flattened ovoid shape, 13.9 mm long, 10.2 mm wide and 8.5 mm thick (Figure 2A). Its mass is 0.94 grams, with a beige exterior color. Its surface is mostly smooth, with granulations in some places. Microscanner analysis (voxel of 8.25 μm , 120 kV acceleration voltage) shows a lighter eccentric nucleus (7.1 mm long) surrounded with several dark coarse-element thick layers, each bordered by a thin, lighter border (Figure 2C).

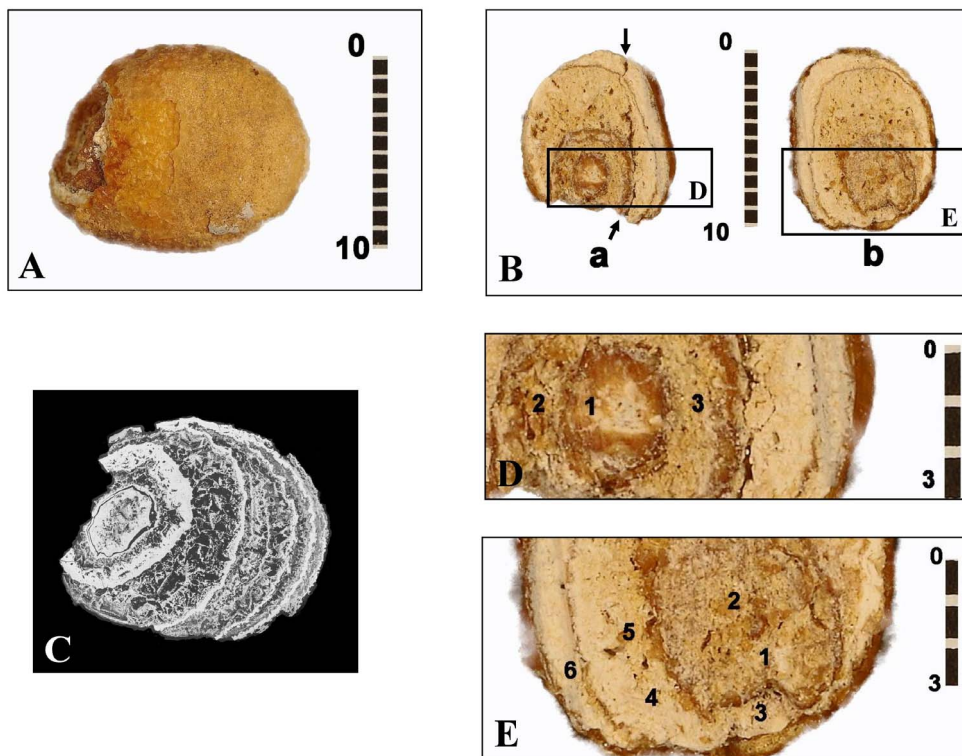


Figure 2. Different views of the bladder stone found in the B1S passage-grave in Chenon (Charente, France). (A) External appearance. (B) Views of the two sections of the bladder stone (section a and section b) showing its nucleus and its various layers. Arrows: break plane for section a. (C) Microtomography of the bladder stone finely pointing its different layers, some thin, others thick with coarse granulation. (D) Enlarged view of part of section a of the bladder stone with the marking of the three areas D1–D3 analyzed by EDX micro-analysis. (E) Enlarged view of part of section b of the bladder stone with the marking of the six areas E1–E6 analyzed by EDX micro-analysis. Scales in mm.

The microelementary analysis EDX study at SEM (25 kV, resolution of 125 eV) of the two intermediate zones, external and internal (Table 1), has revealed the following average concentrations of the main elements: (O) = 43.00%, (C) = 2.52%, (P) = 14.75%, (Ca) = 37.45%, (Al) = 1.30%, (Mg) = 0.71%. Other elements such as Na, Zn, Si, S are also present in smaller proportions, however with a high percentage of error. In the internal structure of the nucleus, a concentration of (O) = 39.14%, (C) = 2.21%, (P) = 15.21%, (Ca) = 41.42%, (Al) = 1.15%, (Mg) = 0.41% shows a little more calcium phosphate in the core than in the outer layers and less CO₃ substitution in the core than in the outer areas. EDX analysis confirms a significant proportion of magnesium in the internal intermediate zone of the stone (Table 1, E5; Figure 3) in proportions which, relative to calcium, are compatible with

whitlockite. A Ca/P ratio has been found around 2.54 for the peripheral areas and around 2.73 for the nucleus (Table 1). Its high value can be explained by the presence of calcite due to a limestone environment. It is indeed a stone of calcium phosphates with as minor elements: sodium, zinc, silicon and sulfur.

FTIR infrared microscopy (Figure 4) is relatively easy to use when using the ATR technique. The ν_1 and ν_2 modes (absorption band at 474 cm⁻¹) of the phosphate anion (PO₄) are only weakly active in infrared. The shoulder, here present at 963–957 cm⁻¹ (ν_1 de PO₄), is typical of phosphate components [58, 59]. The ν_3 and ν_4 of (PO₄) areas, much more intense, are located here (with a shift due to the technique used here) at peaks around 1013 cm⁻¹ (ν_3 of PO₄), 599 cm⁻¹ (ν_4 of PO₄) and 559 cm⁻¹ [60]. The anion (HPO₄)²⁻ shows an IR band at 871 cm⁻¹.

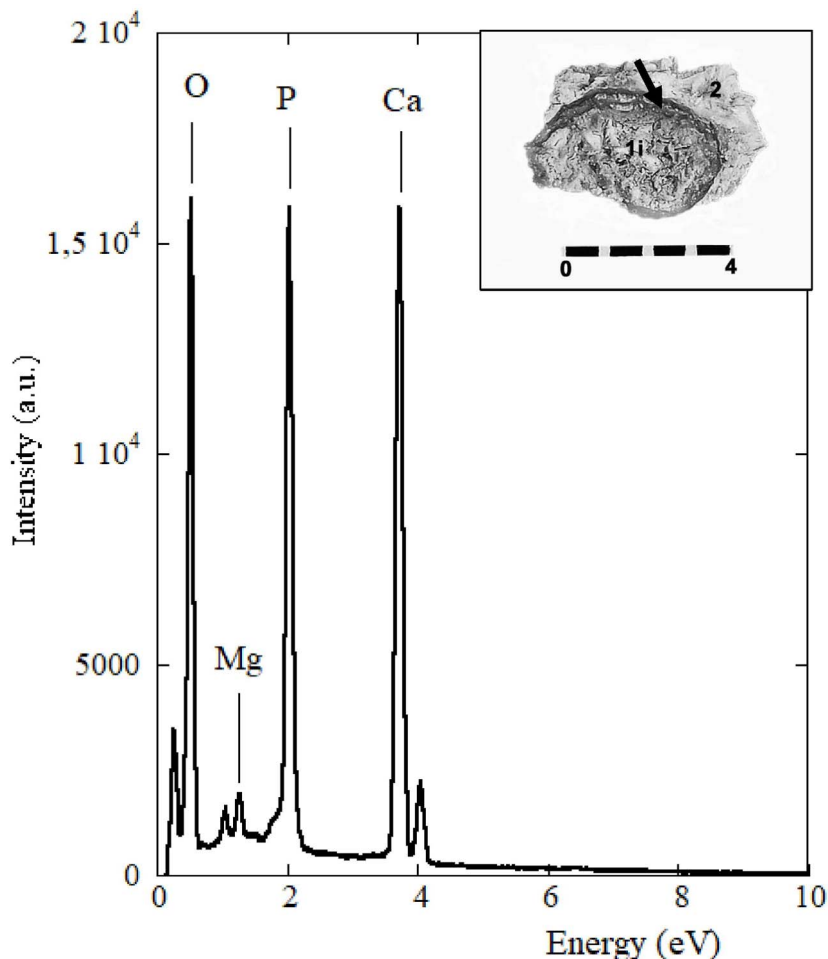


Figure 3. Spectrum of the microchemical EDX analysis of the internal intermediate zone 2 (arrow) close to the stone shell found in the B1S passage-grave in Chenon (Charente, France).

The shift of the peaks means that the peak of carbonates (substituted for hydroxyls in the apatitic structure) is around 1412–1413 cm^{-1} (ν_3 band of $(\text{CO}_3)^{2-}$) and not at 1419–1420 cm^{-1} , and at 871–872 cm^{-1} (bending band ν_4 of $(\text{CO}_3)^{2-}$). We know that proteins are mainly detected by their amide bands I and II around 1550 cm^{-1} and 1650 cm^{-1} (here 1640–1643 cm^{-1}). The absence of infrared vibrations in the 1300–1370 cm^{-1} and 700–800 cm^{-1} regions excludes the presence of calcium oxalates and purines [61].

These FTIR spectra (Figure 4) confirm the preponderant presence in this stone of carboxylate or carbonated apatite of $\text{Ca}_{10}(\text{PO}_4)_6(\text{CO}_3)(\text{OH})_2$ [62] general formula. Lateral inflections of the absorbance peak curve from 1011 cm^{-1} to 1136 and 1078 cm^{-1}

(the latter corresponding to the stretching vibration band HPO_4^{2-}) indicate the presence of whitlockite or mixed phosphate of calcium and hydrated magnesium which has the formula $\text{Ca}_9\text{Mg}(\text{HPO}_4)(\text{PO}_4)_6$ [63,64]. This rare phosphate found in kidney stones is stabilized by incorporating a little magnesium into its structure. Whitlockite has been identified in particular by its vibration at 992 cm^{-1} , on the shoulder of the peak at 1011 cm^{-1} . Another calcium phosphate, amorphous carbonated calcium phosphate ACCP, has been seen on several of the spectra shown here with vibrations at 1064 cm^{-1} and 543 cm^{-1} .

Different biochemical conditions therefore have caused several forms of crystallization during the

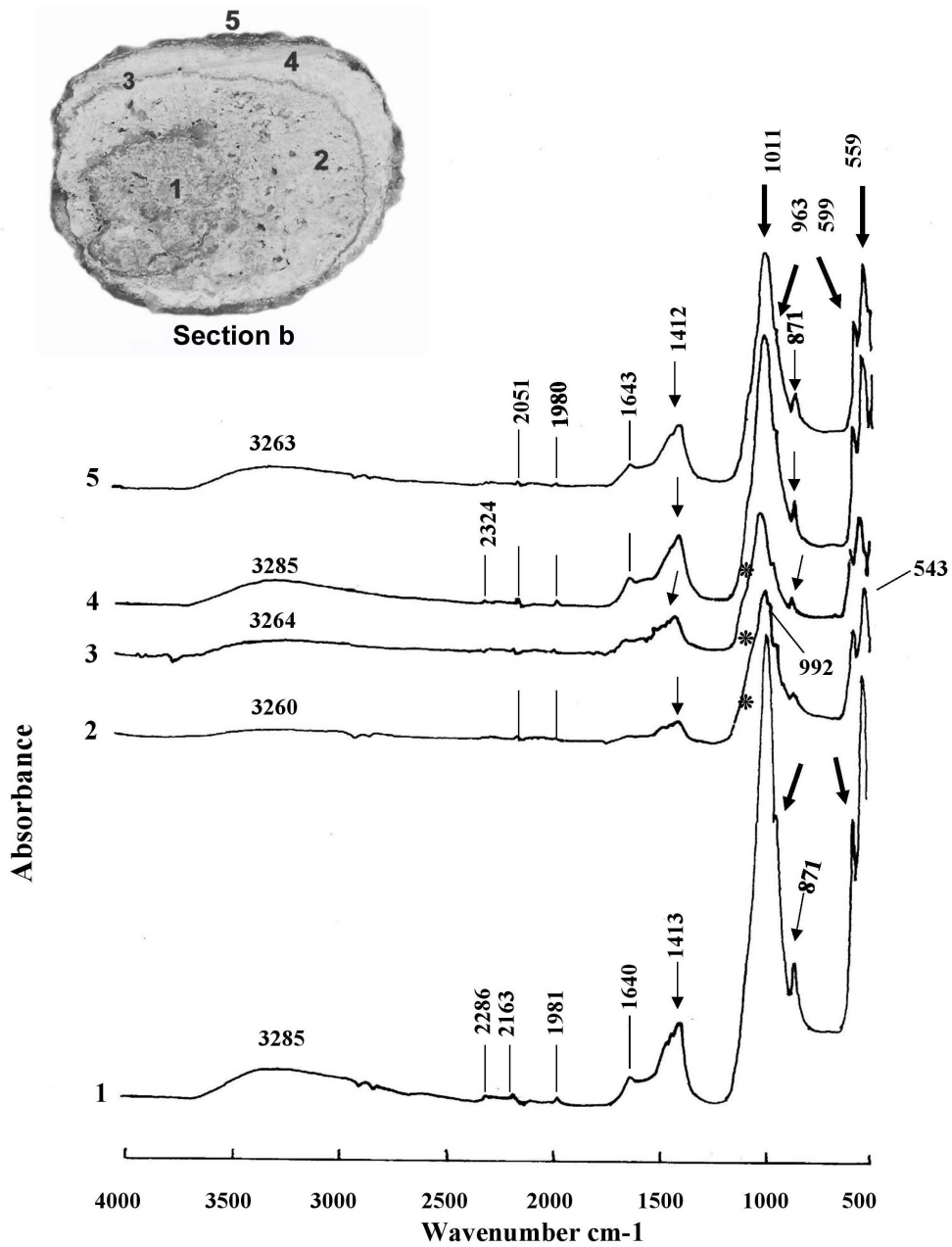


Figure 4. Infrared FT-IR spectra of the five areas analyzed in the section b of the bladder stone of the B1S passage-grave in Chenon (Charente, France) composed of calcium phosphate (carapatite) mixed with whitlockite and amorphous carbonated calcium phosphate ACCP: 1, the nucleus; 2, the internal intermediate zone; 3, the external intermediate thin zone; 4, the external intermediate thick zone; 5, the external layer. Peaks at 1011, 963, 599 and 559 cm^{-1} correspond to phosphate absorptions (thick arrows). Peaks at 1412–1413 and 871 cm^{-1} denote carbonate ions (thin arrows). The stars on the shoulder of the peak at 1011 cm^{-1} indicate whitlockite as well the peak at 992 cm^{-1} . The peak at 543 cm^{-1} indicates the presence of ACCP.

Table 1. Quantitative results in mass percentages of the main chemical elements and secondary elements obtained by EDX analysis of the bladder stone found in the B1S passage-grave in Chenon (Charente, France)

| % mass | | O | C | P | Ca | Al | Mg | Na | Zn | Si | S | Ca/P |
|-----------------------|----|-------|------|-------|-------|------|------|------|------|------|------|------|
| External interm. area | E6 | 41.21 | 3.77 | 14.79 | 37.02 | 2.30 | 0.54 | 0.43 | 0.25 | 0.14 | 0.07 | 2.50 |
| | E5 | 44.47 | 1.75 | 14.80 | 36.82 | 0.80 | 1.05 | 0.00 | 0.21 | 0.06 | 0.04 | 2.49 |
| Internal interm. area | E4 | 40.62 | 1.61 | 15.90 | 39.98 | 0.89 | 0.70 | 0.04 | 0.17 | 0.03 | 0.05 | 2.51 |
| | E3 | 45.55 | 2.95 | 13.50 | 35.97 | 1.19 | 0.53 | 0.00 | 0.14 | 0.10 | 0.06 | 2.66 |
| | E1 | 42.10 | 2.22 | 15.36 | 37.38 | 1.74 | 0.78 | 0.11 | 0.16 | 0.07 | 0.09 | 2.43 |
| Central area | D2 | 34.11 | 1.65 | 14.36 | 47.85 | 0.95 | 0.25 | 0.04 | 0.52 | 0.14 | 0.13 | 3.33 |
| | D3 | 38.01 | 2.26 | 15.55 | 42.86 | 0.75 | 0.24 | 0.04 | 0.14 | 0.08 | 0.07 | 2.76 |
| Nucleus | E2 | 41.95 | 2.54 | 15.01 | 38.63 | 1.18 | 0.34 | 0.12 | 0.09 | 0.11 | 0.05 | 2.57 |
| | D1 | 39.51 | 2.38 | 15.76 | 40.37 | 1.15 | 0.44 | 0.00 | 0.17 | 0.10 | 0.13 | 2.56 |

Refer to Figure 2 for the numbering of the different areas. The highest percentages are shown in red and the lowest in green.

formation of this calculus. It is therefore a mixed stone at least tertiary (with three components, all of a phosphatic nature).

A high carbonation rate $CR = (CO_3)^{2-} / (PO_4)^{3-}$ [28] is an important criterion to be taken into account to suspect the involvement of a urease germ infection in the formation of a stone [65]. Its value is obtained (also called R c/p) by making the ratio of the areas calculated on the IR graph (Figure 4, spectrum 4) located between the vibrations ν_3 of $(CO_3)^{2-}$ from 1530 to 1330 cm^{-1} —here 1412–1417 cm^{-1} —and ν_3 of $(PO_4)^{3-}$ from 1230 to ~ 900 cm^{-1} —here 1011–1017 cm^{-1} — [66]. The high content of carbonate ions (despite the absence of the ν_4 vibration at 712 cm^{-1}) suggests that the sample does not contain (or very little) calcium carbonate, but that the carbonate ions have been incorporated into the apatite during crystallization. This carbonate content reaches 25% in the carapatite of the peripheral layers of the B1S dolmen calculus at Chenon and 17% in its core, which certainly makes it an infection stone.

SEM investigation may show carapatite spherules associated with rhombohedral whitlockite crystals and granules of amorphous carbonate calcium phosphate. Pictures taken inside the peripheral layers of this stone (Figure 5) made it possible to identify these small spheres of agglomerated carapatite filaments with an average diameter of 2.72 μm (range 1.76 μm to 3.57 μm). It appears that the carapatite spherules have a smaller diameter in males

(3.4 \pm 1.8 μm) than in females (5.7 \pm 3.9 μm), but the range of measurements prevents it from being asserted [28].

Bacterial imprints can be seen with SEM on the surface of carapatite spherules [28], either in the form of rods (*Proteus sp.* or *Klebsiella sp.*) or in round prints indicating the ancient presence of *Cocci* such as *Staphylococcus sp.* [67,68]. The search for bacterial imprints in these spherules has been carried out in our case without convincing results (Figure 5).

5. Discussion

The diagnosis of bladder stones is immediately confirmed in our study by the concentric arrangement of the different layers [69–71] and by the alternation in these layers of crystalline and microcrystalline [72] that is typical of phosphate urinary lithiases, well observed on micro-scan (Figure 2C). A study of the chemical composition of kidney stones is important to understand how they formed. It is widely accepted that different areas of a stone should be analyzed separately. Laser Induced Breakdown Spectroscopy (LIBS) technology that is not used for our stone appears to be currently the most appropriate method to perform a rapid and simultaneous multi-elemental analysis of each part of a urinary stone, as it does not damage the sample, and, in addition, some of these analyzers are portable [45]. However, unlike infrared spectrophotometry, this technique does not give the

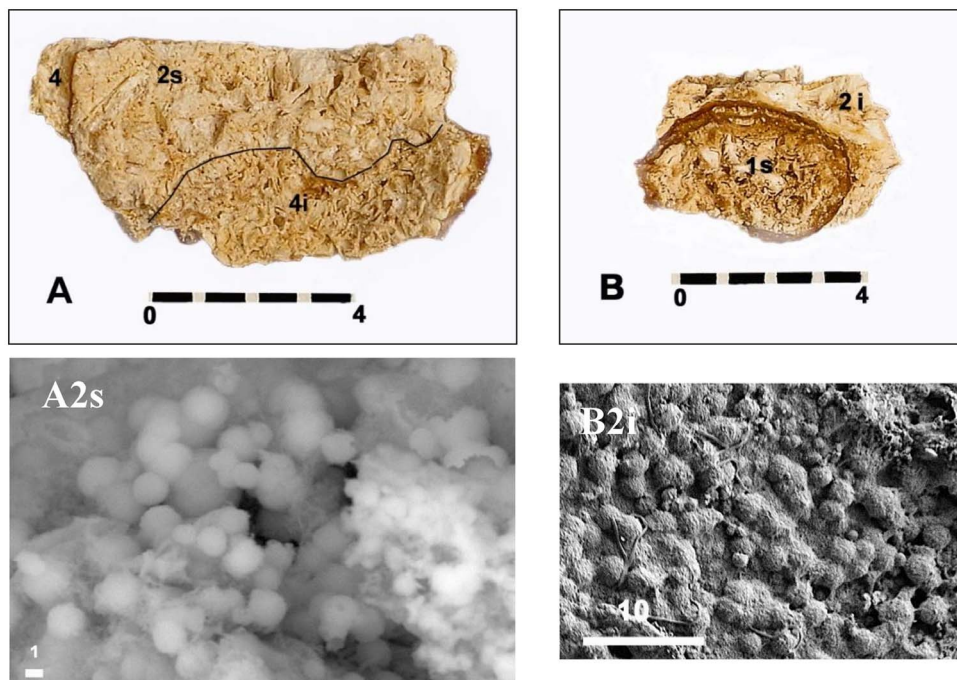


Figure 5. Internal views (A, B) of two fragments of the fracture plane of half a of Chenon's B1S bladder stone. (A2s) Spherules of carapatite without any bacterial imprints magnified 4000 \times observed at the level of the upper part of the internal intermediate zone 2. (B2i) Spherules of carapatite without any bacterial imprints magnified 1000 \times observed at the level of the lower part of the internal intermediate zone 2 located in contact with the surface of the core 1. Scales in mm (A, B) and in μm (A2s, B2i).

molecular and crystalline composition of the samples and therefore cannot replace infrared analysis (or X-ray diffraction) of the samples whose nature we want to identify precisely.

The presence of three calcium phosphates, two of which are highly carbonated, points to an infectious cause for the formation and growth of this stone. Usually, this lithogenesis results in the presence of a fourth phosphate, struvite (ammonium magnesium phosphate hexahydrate) which was not detected here. It should be noted that when stones have been stored for a long time in the air (which is our case), struvite tends to degrade and disappear [73]. The high carbonate content (between 17 and 25%) suggests lithogenesis into alkaline urine under the dependence of ureolysis by bacteria that possess urease. Elevation of urine pH above 6.8 (alkaline or weakly acidic urine) promotes oxidation of CO_2 to carbonate (CO_3)²⁻ and then its precipitation as carbonate-apatite or carapatite [74,75]. Carapatite appears to be more abundant in the stones of

women than in those of men, who more frequently produce stones composed mainly of calcium oxalate dihydrate [65].

Nowadays, seven major types of calculi are distinguished according to their crystalline composition [24,76]. The Chenon B1S stone studied here, falls into Daudon's type IVb [24] since it includes at least three phosphates : carapatite, amorphous carbonate calcium phosphate PACC and whitlockite (calcium magnesium hydrogen phosphate of chemical formula $\text{Ca}_9\text{Mg}(\text{HPO}_4)(\text{PO}_4)_6$). The morphological details and chemical compositions of a number of ancient bladder stones have been surveyed by Steinbock [8]. His table has been repeated and expanded (Table 2; [7,9,10,15,22,23,77-91]).

EDX analysis established that the basic structure of our calculation was calcium and phosphorus. The high Ca/P value found for our example has been reported several times: for a predominantly calcium phosphate bladder stone (with calcium carbonate and some calcium oxalate) collected from a tomb in

Table 2. Some examples of kidney and bladder stones found in excavations in Africa, America and Europe (shaded) in burials dated to prehistoric and early historical times (after Steinbock, [8], completed)

| Location | Sex/Age | Size-type | Composition | Date [reference] |
|---------------------------------|----------|---|----------------------------------|---------------------------|
| Uzzo, Trapani, Sicily, Italy | F/20–25 | | Carbonate Phosphate | 8500 BC [9,10] |
| El Amrah Egypt | M/16 | 65 mm Bladder | Urate | 3500 BC [77,78] |
| Egypt | — | 45 × 30 mm 40 × 25 mm, Bladder | Urate, Mg Ammon., Phosph. | 3500 BC [79] |
| Indian Knoll Kentucky, USA | M/24 | 40 × 27 × 23 mm Bladder | Oxalate | 3300 BC [80] |
| Helouan Egypt | — | 35 × 30 mm (5 kidney stones) 30 × 20 mm, Renal? | — | 3100 BC [81] |
| Chenon B1S Charente, France | M? | 14 × 10 × 8.5 mm Bladder | Carbapatite Whitlockite, CCPA | Ille millenium BC [23] |
| Naga-el-Dier Egypt | — | 16 mm (4 kidney stones), Renal | Oxalate Phosphate | 2800 BC [77] |
| Egypt | F/35 | Renal pelvis Renal | Carbonate Phosphate | 2650–2150 BC [82,83] |
| Prayssac, Lot France | Adult | 41 × 35 × 30 mm Bladder | Phosphate | 2200 BC [22] |
| Yorkshire England | Adult | 40 × 30 × 30 mm Bladder | — | 2000–700 BC [84] |
| Fulton County Illinois, USA | F/20–22 | 17 × 10 × 7 mm Renal | Apatite Struvite | 1500 BC [15] |
| Csongr d-Felgyd Hungary | F/Adult | 35 × 34 × 30 mm Bladder? | Oxalate, Sulfate Ammon. Mg | 1800–500 BC [85] |
| Arizona USA | ?/18 | 42 × 34 × 27 mm Bladder | Carbonate Phosphate, Urate | <1100 BC [86] |
| Egypt | M/Adult | Bladder | — | 1000 BC [87] |
| Sudan | 32 cases | 30 × 39 mm Bladder | Calcite Apatite | 1000 BC [88] |
| Schleswig Germany | M/40–50 | 11 × 11 mm 4 × 4 mm, Renal? | Apatite | 500–250 BC [89] |
| Northeast Arizona USA | M/> 30 | 30 × 27 × 25 mm Bladder | Oxalate, Struvite Phosphate | 500–750 AD [7] |
| Sz kkutas-K polna Hungary | M/41–50 | 50 × 40 × 35 mm Bladder | Carbonate Apatite | 700–800 AD [90] |
| Oluz H y k Turkey | F/59–71 | 65 × 45 mm Bladder | Phosphate | 11th Century [91] |

the medieval cemetery of Gdańsk, Poland (2.23 for the outer layers and 1.99 for the inner layers) [4]; for the hydroxyapatite bladder stone of a 59–71 year old woman who lived in the XIth century in Ol z H y k, Turkey (2.47 for the cortex and 2.54 for the core) [91].

Water infiltration into a non-hermetic grave can have several consequences on the chemical analysis of a stone, either enrichment in calcium carbonate or dissolution of phosphate ions if the water is acidic. This was reported for a bladder stone dated to 700–800 AD found in a 41–50 year old man in Sz kkutas-K polna, Hungary [90]. The core was dissolved. It was the same for another adult female bladder stone dated to the 9th–7th millennia BC buried in an oval pit filled with soil and limestone blocks that was found in the Uzzo Cave in Italy. Chemical analysis yielded a significant amount of calcium carbonate with small amounts of phosphate components [10]. The consequence was a Ca/P ratio of more than 6 both at the periphery of the stone and in its core.

Many discoveries of oxalate stones have been made inside mummies—especially Egyptian—but also in pre-Columbian tombs, to mention the most frequent cases. The size of these stones can vary up to that of a golf ball [92]. Without contact with the outside world, these mummies perfectly preserve all the components of the stones. This is the case of a naturally dehydrated mummy, dated from 500 to 750 AD, discovered in Arizona wrapped in a fabric decorated with furs and feathers, which could be fully studied in 1979 [7]. The bladder stone was still in the contracted bladder. Its complete chemical composition was calcium oxalate monohydrate in monoclinic crystals (75%), magnesium oxalate (9%), struvite in orthorhombic crystals (6%), calcium phosphate (4%), ammonium acid urate (2%) and silicon dioxide (1%). This complete analysis shows an absence of pollution. Another mummy of an adult woman, dated to the beginning of the 19th century, found in a rough wooden coffin in the church of Borgo Cervato in Umbria (Italy), had a bladder stone of 7.5 cm in diameter, the outer layers of which were composed of crystallized struvite and the inner layers of acid ammonium urate. The Ca/P ratio was only 0.6 for the outer layers and 1.6 for the inner layers [92]. Fortunately the mummy was in a cool place away from light, which allowed the struvite not to disappear, when it is known that a poor storage condition

(e.g., high temperature in summer in a warehouse) can lead to its disappearance [73].

The calculation of the carbonation rate for our stone and the observation of carbapatite spherules have allowed us to affirm that the stone found in the B1S passage-grave of Chenon had a bacterial origin without it being possible for us to observe impressions with certainty. Only a few structures with pores of about 2 μm , compatible with cocci, but not bacilli, were observed locally. The relationship between bacteria and urinary stones has been documented since the time of Hippocrates [93]. An important contribution to understanding the origin of infection stones was made by Brown [93]. He was the first to put forward the theory that bacteria split the urine and thus cause the formation of stones. At the same time, he isolated *Proteus vulgaris* from a stone nucleus, although the genus *Proteus* had first been described by Hauser as early as 1885 [94]. In 1925, Hager and Magath [95] suggested the enzyme “urease” as the cause of hydrolysis of urine into ammonia and carbonic acid. A year later, Sumner [96] succeeded in isolating the enzyme from *Canavalia ensiformis*. Nowadays, more than 200 species of bacteria show urease activity using urea as a nitrogen source [97].

The most important urease-producing pathogens are: *Proteus*, *Klebsiella*, *Pseudomonas* and several species of *Staphylococcus* [98]. However, the *Proteus* group is the main culprit in infection stones [99,100]. Over 90% of its strains possess a highly active urease. They are widespread saprophytic bacteria in soil and water. *Proteus* is known as an opportunistic bacterial pathogen. The essential characteristic of *Proteus* bacteria is a swarming phenomenon, a process of multicellular differentiation of short rods into elongated swarm cells [100].

A large number of trace elements have been quantitatively detected in kidney stones [45,101,102]. The first paper on trace elements in urine was published in 1963 [103]. Their influence on the crystallization process in stones was recognized in the following years [104,105]. Food intake, metabolism and the role of the environment explain their presence. Many of these trace elements are known to be essential in specific metabolic processes [106]. A few trace elements such as zinc and magnesium are thought to have an inhibitory effect on urinary lithiasis [107]. A high proportion of zinc and strontium has been found in calcium phosphate stones [108] and a correlation

between the two of them [109]. Authors believe that zinc may play a role in the formation of the stone core [106,110,111]. However, the role of zinc in lithogenesis remains unclear. The presence of whitlockite in our stone, which is very rare in the urinary system, can be explained by the traces of zinc found in the EDX analysis because zinc stabilizes this phosphate, and it should not be forgotten that zinc is found in significant amounts in the nearby prostate, if it is a male [112].

6. Conclusion

This investigation confirms once again that FTIR micro-spectrometry offers multiple advantages for the identification and quantification of the mineral phase of the constituents of bladder stones, and this in a non-destructive manner, which is an advantage in archaeology.

The combined use of FTIR spectroscopy by ATR with EDX chemical micro-analysis and SEM observation of crystalline constituents as well as bacterial fingerprints at the origin of urolithiasis, show their effectiveness in the analysis of bladder stones. The stone studied here, which is dated to the Final Neolithic period, was found in a multiple grave in the Chenon Necropolis and belonged to an individual (a man?) who had a possibly recurrent urinary tract infection due to a urease bacterium (probably not from the *Proteus sp.* group).

This study has also made it possible to draw the attention of any searcher to the possibility of discovering extra-skeletal objects accompanying the skeletal remains of prehistoric and ancient burials. Everyone must consider that there are several steps for an archaeologist or anthropologist researcher to make a diagnosis on a biological object recovered in excavation [91]. First, defining the location of the object among the exposed human body; second, determining the type of calcification if possible *in situ*; third, working to identify the mineralogy and elementary compositions of the object to define possible causes. Thus, discoveries of this type may multiply and provide new, well-documented evidence to the history of diseases in past populations.

And in the case of the discovery of a biological object resembling a urolithiasis, we have to make sure that it is put in a hermetic box, protected from light and cool [73]. In this way, discoveries of this type

can be multiplied, analyzed in good conditions and bring new well documented evidence to the history of diseases in past populations.

Conflicts of interest

Authors have no conflict of interest to declare.

Acknowledgments

The main author (GRC) thanks Messrs Gr gory Hauss and Philippe Legros, research engineers at PLACAMAT in Pessac (Gironde, France), for their competence and efficiency in handling the micro-scanner and the SEM-EDX.

References

- [1] C. A. Baud, C. Kramar, *Bull. M m. Soc. Anthropol. Paris*, 1990, **2**, 163-170.
- [2] D. Komar, J. E. Buikstra, *Int. J. Osteoarchaeol.*, 2003, **13**, 157-164.
- [3] G. Fornaciari, V. Giuffr , *Pathobiology*, 2012, **79**, 257-267.
- [4] J. J. Gladykowska, D. Nowakowski, *PLoS One*, 2014, **9**, 1-6.
- [5] G. Cole, C. Rando, L. Sibun, T. Waldron, *J. Paleopathol.*, 2015, **10**, 51-57.
- [6] B. Kwiatkowska, A. Bisiecka, L. Pawelec, A. Witek, J. Witan, D. Nowakowski, *PLoS One*, 2021, **16**, 1-16.
- [7] J. M. Streitz, A. C. Aufderheide, M. El Najjar, D. Ortner, *J. Urol.*, 1981, **126**, 452-453.
- [8] R. T. Steinbock, *J. Paleopathol.*, 1989, **3**, 39-59.
- [9] M. Piperno, *Kokalos*, 1976, **XXII-XXIII**, 798-816.
- [10] A. d'Alessio, E. Bramanti, M. Piperno, G. Naccarato, P. Vergamini, *Archaeometry*, 2005, **47**, 127-136.
- [11] W. H. Wollaston, *Philos. Trans.*, 1797, **87**, 386-401.
- [12] M. L pez, B. Hoppe, *Pediatr. Nephrol.*, 2010, **25**, 49-59.
- [13] M. E. Salem, G. Eknoyan, *Am. J. Nephrol.*, 1999, **19**, 140-147.
- [14] T. Bardin t, *Les papyrus m dicaux de L'Egypte Ancienne*, Fayard, Paris, 1995.
- [15] C. W. Beck, W. P. Mulvaney, *JAMA*, 1966, **195**, 1044-1045.
- [16] V. A. Master, M. V. Meng, M. L. Stoller, in *Urinary Stone Disease. The Practical Guide to Medical and Surgical Management* (M. L. Stoller, M. V. Meng, eds.), Wiley-Blackwell, 2007, 3-26.
- [17] W. G. Robertson, *Br. J. Urol.*, 1978, **50**, 449-454.
- [18] V. Giuffr , L. Ventura, S. Minozzi, A. Lunardini, R. Quaresina, *Am. J. Med.*, 2011, 1186-1187.
- [19] Ch. L. Prince, P. L. Scardino, C. T. Wolan, *J. Urol.*, 1956, **75**, 209-215.
- [20] W. G. Robertson, M. Peacock, P. J. Heyburn, F. A. Hanes, *Scand. J. Urol. Nephrol.*, 1980, **Suppl. 53**, 15-30.
- [21] H. Duday, *The Archaeology of the Dead: Lectures in Archaeoethanatology*, Oxbow Books, Oxford, UK, 2009, 85-88 pages.

- [22] H. Duda, J. Clottes, H. Mercadier, F. Rouzaud, J. Zammit, "Un calcul urinaire provenant du dolmen de la Bertraundoune à Prayssac (Lot, France)", in *Actes du 3^{ème} Congrès Européen de l'Association de Paléopathologie, Caen (France), Condé-sur-Noireau* (Collectif, ed.), 1980, 87-90.
- [23] G. R. Colmont, *Ann. Soc. Sci. Nat. Charente-Marit.*, 2016, **X**, 791-824, Museum La Rochelle.
- [24] M. Daudon, C. A. Bader, P. Jungers, *Scanning Microsc.*, 1993, **7**, 1081-1104.
- [25] M. Daudon, *Arch. Pédiatr.*, 2000, **7**, 855-865.
- [26] M. Daudon, H. Bouzidi, D. Bazin, *Urol. Res.*, 2010, **38**, 459-467.
- [27] M. Daudon, A. Dessombz, V. Frochot, E. Letavernier, J.-Ph. Haymann, P. Jungers, D. Bazin, *C. R. Chim.*, 2016, **19**, 1470-1491.
- [28] X. Carpentier, M. Daudon, O. Traxer, P. Jungers, A. Mazouyes, G. Matzen, E. Véron, D. Bazin, *Urology*, 2009, **73**, 968-975.
- [29] D. Bazin, G. André, R. Weil, G. Matzen, E. Véron, X. Carpentier, M. Daudon, *Urology*, 2012, **79**, 786-790.
- [30] E. Gauron, J. Massaud, *XVIII^e supplément à Gallia-Préhistoire*, Editions du CNRS, Paris, 1983, 85-119 pages.
- [31] J. Guilaine, in *Archéologie de la France : le Néolithique* (J. Tarrête, Ch.-T. Le Roux, eds.), Editions A. et J. Picard, Paris, 2008, 9-30.
- [32] E. Crubézy, P. Sellier, *Bull. Mém. Anthropol. Paris*, 1990, **2**, 171-177.
- [33] S. Mays, *The Archaeology of Human Bones*, Routledge, London and New York, 1998, 143 pages.
- [34] P. L. Walker, R. R. Bathurst, R. Richman, T. Gjerdrum, V. A. Andrushko, *Am. J. Phys. Anthropol.*, 2009, **139**, 109-125.
- [35] A. H. Goodman, J. C. Rose, *Yearb. Phys. Anthropol.*, 1990, **33**, 59-110.
- [36] M. Skinner, *J. Archaeol. Sci.*, 1996, **23**, 833-852.
- [37] L. Alvesalo, *Hum. Genet.*, 1997, **101**, 1-5.
- [38] E. MacLellan, *TOTEM*, 2005, **13**, 41-52.
- [39] A. H. Goodman, G. J. Armelagos, J. C. Rose, *Hum. Biol.*, 1980, **52**, 515-528.
- [40] K. M. Lamphear, *Am. J. Phys. Anthropol.*, 1990, **81**, 35-43.
- [41] N. J. Malville, *Am. J. Phys. Anthropol.*, 1997, **102**, 351-367.
- [42] M. Slaus, *Am. J. Phys. Anthropol.*, 2000, **111**, 193-209.
- [43] D. H. Temple, M. Nakatsukasa, J. N. McGroarty, *J. Archaeol. Sci.*, 2012, **39**, 1634-1641.
- [44] D. J. Reid, M. C. Dean, *Am. J. Phys. Anthropol.*, 2000, **113**, 135-139.
- [45] V. K. Singh, P. K. Rai, *Biophys. Rev.*, 2014, **6**, 291-310.
- [46] F. Brisset, M. Repoux, J. Ruste, F. Grillon, F. Robaut, *Microscopie électronique à balayage et microanalyses*, EDP Sciences, Paris, 2009.
- [47] D. Bazin, M. Daudon, *Ann. Biol. Clin.*, 2015, **73**, 517-534.
- [48] D. Bazin, E. Boudierlique, M. Daudon, V. Frochot, J.-Ph. Haymann, E. Letavernier, F. Tielens, R. Weil, *C. R. Chim.*, 2022, **25**, no. S1, 37-60.
- [49] N. Quy Dao, M. Daudon, *Infrared and Raman Spectra of Calculi*, Elsevier, Paris, 1997.
- [50] M. Daudon, D. Bazin, *C. R. Chim.*, 2016, **19**, 1416-1423.
- [51] M. Daudon, D. Bazin, "New techniques to characterize kidney stones and Randall's plaque", in *Urolithiasis: Basic Science and Clinical Practice* (J. J. Talati, H. G. Tiselius, D. M. Albalá, Z. Ye, eds.), Springer, 2012, 683-707.
- [52] D. Bazin, E. Letavernier, J.-P. Haymann, P. Méria, M. Daudon, *Prog. Urol.*, 2016, **26**, 608-618.
- [53] D. Bazin, M. Daudon, *J. Spect. Imaging*, 2019, **8**, article no. a16.
- [54] A. Dessombz, P. Méria, D. Bazin, M. Daudon, *PLoS One*, 2012, **7**, article no. e51691.
- [55] A. Dessombz, P. Méria, D. Bazin, E. Foy, S. Rouzière, R. Weil, M. Daudon, *Prog. Urol.*, 2011, **21**, 940-945.
- [56] C. J. Cros, D. Bazin, A. Kellum, V. Rebours, M. Daudon, *C. R. Chim.*, 2016, **19**, 1642-1664.
- [57] M. G. Baron, N. Benmoussa, D. Bazin, I. Abadie, M. Daudon, P. Charlier, *Urolithiasis*, 2018, **47**, 487-488.
- [58] A. Hess, W. Hicking, W. Vahlensieck, *GIT-Labor-Medizin*, 1981, **1**, 19-25.
- [59] A. Hess, G. Sanders, *Atlas of Infrared Spectra for the Analysis of Urinary Concrements*, Georg Thieme Verlag, Stuttgart, 1988.
- [60] D. Bazin, M. Daudon, *Ann. Biol. Clin.*, 2015, **73**, 517-534, John Libbey Eurotext.
- [61] I. Petit, G. D. Belletti, T. Debroise, M. J. Llansola-Portoles, I. T. Lucas, C. Leroy, C. Bonhomme, L. Bonhomme-Coury, D. Bazin, M. Daudon, E. Letavernier, J. Ph. Haymann, V. Frochot, F. Babonneau, P. Quaino, F. Tielens, *ChemistrySelect*, 2018, **3**, 8801-8812.
- [62] T. White, C. Ferraris, J. Kim, S. Madhavi, *Rev. Mineral. Geochem.*, 2005, **57**, 307-401.
- [63] P. Carmona, J. Bellanato, E. Escolar, *Biospectroscopy*, 1997, **3**, 331-346.
- [64] D. Bazin, R. J. Papoular, E. Elkaim, R. Weil, D. Thiaudière, C. Pisapia, B. Ménez, N. S. Hwang, F. Tielens, M. Livrozet, E. Boudierlique, J.-Ph. Haymann, E. Letavernier, L. Hennem, V. Frochot, M. Daudon, *C. R. Chim.*, 2022, **25**, no. S1, 343-354.
- [65] L. Maurice-Estépa, P. Levillain, B. Lacour, M. Daudon, *Scand. J. Urol. Nephrol.*, 1999, **33**, 299-305.
- [66] A. Grunenwald, Ch. Keyser, A.-M. Sautereau, E. Crubézy, B. Ludes, *J. Archaeol. Sci.*, 2014, **49**, 134-141.
- [67] L. Cifuentes Delatte, M. Santos, *Eur. Urol.*, 1977, **3**, 96-99.
- [68] L. Cifuentes Delatte, *Composición y estructura de los cálculos renales*, Salvat Editores, Barcelona, 1984.
- [69] H. J. Rodgers, R. G. Spector, J. R. Trounce, *A Textbook of Clinical Pharmacology*, Hodder and Stoughton, London, 1981.
- [70] T. Anderson, *Br. J. Urol. Int.*, 2001, **88**, 351-354.
- [71] T. Anderson, *Int. J. Osteoarchael.*, 2003, **13**, 165-167.
- [72] M. G. Baron, N. Benmoussa, D. Bazin, I. Abadie, M. Daudon, P. Charlier, *Urolithiasis*, 2018, **47**, 487-488.
- [73] J. C. Williams Jr, A. J. Sacks, K. Englert, R. Deal, T. L. Farmer, M. E. Jackson, J. E. Lingeman, J. A. Mc Ateer, *J. Endourol.*, 2012, **26**, 726-731.
- [74] A. Hess, W. D. Miersch, *Int. Urol. Nephrol.*, 1989, **21**, 257-267.
- [75] T. Deguchi, T. Yoshida, T. Miyazawa, M. Yasuda, M. Tamaki, H. Ishiko, S. Maeada, *Sex. Transm. Dis.*, 2004, **31**, 192-195.
- [76] M. Daudon, O. Traxer, P. Jungers, *Médecine-Sciences*, Lavoisier, Paris, 2012.
- [77] S. G. Shattock, *Transactions of the Pathological Society of London*, vol. 56, Adlard and Son, London, 1905, 275-290 pages.
- [78] G. Elliot Smith, *The Ancient Egyptians and the Origin of Civilization*, Harper & Brother, London/New York, 1911.
- [79] M. A. Ruffer, *Cairo Sci. J.*, 1910, **4**, 1-5.

- [80] H. W. Smith, *Anthropology*, 1948, **4**, 511-513.
- [81] J. Bitschai, *Am. J. Surg.*, 1952, **83**, 215-224.
- [82] R. Boano, E. Fulcheri, R. Grilletto, E. Leospo, E. Rabino Massa, in *Egyptology at the Dawn of the Twenty-first Century, vol 3: Proceedings of the Eighth International Congress of Egyptologists, Il Cairo 2000, 138(4)* (Z. Hawass, ed.), The American University in Cairo Press, Cairo, New York, 2003, 138-144.
- [83] E. Fulcheri, R. Grilletto, *Paléobios*, 1988, **5**, 61-63.
- [84] J. R. Mortimer, *Forty Year's Researches in British and Saxon Burial Mounds of East Yorkshire*, A. Brown and Sons Limited, London, 1905.
- [85] M. M. Boross, J. Nemeskeri, *Homo*, 1963, **14**, 149-150.
- [86] G. D. Williams, *JAMA*, 1926, **87**, 941.
- [87] G. E. Smith, W. R. Dawson, *Egyptian Mummies*, George Allen & Unwin, London, 1924.
- [88] D. R. Brothwell, A. T. Sandison (eds.), *Diseases in Antiquity: A Survey of the Diseases, Injuries and Surgery of Early Populations*, Charles Thomas, Springfield, Illinois, 1967, 349-351 pages.
- [89] H. Schutkowski, S. Hummel, S. Gegner, *Paleopathol. Newsl.*, 1986, **55**, 11-12.
- [90] F. Szalai, E. Javor, *Int. Urol. Nephrol.*, 1987, **19**, 151-157.
- [91] K. Özdemir, A. A. Akyolb, Y. S. Erdal, *Int. J. Osteoarchaeol.*, 2015, **25**, 827-837.
- [92] V. Giuffra, L. Costantini, L. Costantini Biasini, D. Caramella, G. Fornaciari, *Urology*, 2008, **72**, 780-781.
- [93] T. R. Brown, *JAMA*, 1901, **36**, 1395-1397.
- [94] G. Hauser, *Über Fäulnisbakterien und deren beziehungen zur septicämie. Ein betrag zur morphologie der spaltpilze*, F.C.W. Vogel, Leipzig, 1885.
- [95] B. H. Hager, T. B. Magath, *JAMA*, 1925, **85**, 1352-1355.
- [96] J. B. Sumner, *J. Biol. Chem.*, 1926, **69**, 435-441.
- [97] R. J. C. MacLean, J. C. Nickel, K.-J. Cheng, J. W. Costerton, *Crit. Rev. Microbiol.*, 1988, **16**, 37-79.
- [98] D. P. Griffith, C. A. Osborne, *Miner. Electrolyte Metab.*, 1987, **13**, 278-285.
- [99] D. P. Griffith, *Kidney Int.*, 1978, **13**, 372-382.
- [100] A. Rózsalski, A. Torzewska, M. Moryl, I. Kwil, A. Maszewka, K. Ostrowska, D. Drzewiecka, A. Zablotni, A. Palusiak, M. Siwinska, P. Staczek, *Folia Biologica Oecologica*, 2012, **8**, 1-17, Acta Universitatis Lodzianensis.
- [101] B. Hannache, A. Boutefnouchet, D. Bazin, M. Daudon, E. Foy, S. Rouzière, A. Dahdouh, *Prog. Urol.*, 2015, **25**, 22-26.
- [102] S. Rouzière, D. Bazin, M. Daudon, *C. R. Chim.*, 2016, **19**, 1404-1415.
- [103] Z. Nagy, E. Szabó, M. Kelenhegyi, *Z. Urol.*, 1963, **56**, 185-190.
- [104] E. Eusebio, J. S. Elliot, *Invest. Urol.*, 1967, **4**, 431-435.
- [105] D. J. Sutor, *Br. J. Urol.*, 1969, **41**, 171-178.
- [106] A. Hesse, R. Siener, in *Urolithiasis* (J. J. Talati, F. Abbas, eds.), Springer, London, 2012, 227-230.
- [107] I. H. Atakan, M. Kaplan, G. Seren, T. Aktoz, H. Gül, O. Inci, *Int. Urol. Nephrol.*, 2007, **39**, 351-356.
- [108] D. Bazin, P. Chevallier, G. Matzen, P. Jungers, M. Daudon, *Urol. Res.*, 2007, **35**, 179-184.
- [109] M. Słojewski, B. Czerny, K. Safranow, K. Jakubowska, M. Olaszewska, A. Pawlik, A. Gołąb, M. Drożdżik, D. Chlubek, A. Sikorski, *Biol. Trace Elem. Res.*, 2010, **137**, 301-316.
- [110] S. M. Lin, C. L. Tseng, M. H. Yang, *Int. J. Rad. Appl. Instrum. A*, 1987, **38**, 635-639.
- [111] V. K. Singh, A. K. Rai, P. K. Rai, P. K. Jindal, *Lasers Med. Sci.*, 2009, **24**, 749-759.
- [112] V. A. Master, M. V. Meng, M. L. Stoller, in *Urinary Stone Disease. The Practical Guide to Medical and Surgical Management* (M. L. Stoller, M. V. Meng, eds.), Humana Press Inc., San Francisco, 2007, 3-26.